Original Article
The role of RhoA/ROCK singal pathway in cardiac rupture after infarction

Lina Hao, Chunping Kang

Department of Gerontology, Xi'an Central Hospital, Xi'an 710003, Shaanxi, China

Abstract: Cardiac rupture is one severe complication of acute myocardial infarction (AMI). The RhoA/ROCK signal protein is up-regulated after AMI, for regulating myocardial injury and fibrosis via inflammation or cytokines. This study observed RhoA/ROCK signal pathway in AMI aged mice, in an attempt to investigate the effect of RhoA/ROCK inhibitor on cardiac rupture after AMI in aged mice, and related mechanisms. Male C57BL/6 mice (18 months old) were assigned into sham, model and inhibitor groups (N=90 each). AMI model was generated by ligation of left coronary artery. Hemodynamics and cardiac ultrasound were examined at day 7, to observe left ventricular remodeling and the rate of cardiac rupture. HE staining was employed to observe myocardial morphology. Serum levels of interleukin-6 (IL-6), tumor necrosis factor-α (TNF-α) were quantified by ELISA at 3, 7 and 14 days after AMI. Protein levels of ROCK1, RhoA, nuclear factor (NF)-κBp65 and transformation growth factor (TGF)-β1 were measured by Western blotting. AMI model group had contraction dysfunction and ventricle dilation, along with elevated IL-6 and TNF-α levels, as well as higher ROCK1, RhoA, NF-κBp65 and TGF-β1 levels (P<0.05 compared to control group). Inhibitor group had lower rate of cardiac rupture, alleviated contraction disorder, ventricle dilation, or myocardial injury, lowered IL-6, TNF-α, ROCK1, RhoA, NF-κBp65 and TGF-β1 expression (P<0.05 compared to model group). RhoA/ROCK pathway might be related with cardiac rupture after AMI. Its inhibitor might decrease cardiac rupture via depressing signal activity, and lowering expression of pro-inflammatory and pro-fibrosis factors.

Keywords: Myocardial infarction, ROCK, RhoA, cardiac rupture

Introduction

Acute myocardial infarction (AMI) can cause hypoxia and insufficient perfusion of myocardial tissues, leading to secondary responses including oxidative stress, inflammation and cell apoptosis, thus severely affecting left ventricular remodeling and cardiac reconstruction. Both ventricular remodeling and cardiac rupture are severe complications of AMI. Among these, cardiac rupture occupies about 20%~31% of total in-patient death after AMI [1, 2]. The clinical symptom of cardiac rupture depends on the site of onset. It usually occurs within 7 days of primary AMI. Independent risk factors of cardiac rupture include aging and gender [3, 4], as it frequently occurs in female aged people of latent myocardial re-perfusion, left ventricular infarction and AMI complicated with hypertension. Currently the mechanism of cardiac rupture after AMI is still unclear [5, 6]. Some studies believed that myocardial remodeling deficits might lead to cardic rupture. Post-

AMI myocardial repair, inflammatory response, injury of extracellular matrix and cell apoptosis all play important roles in cardiac rupture, which is related with cell apoptosis, genetic susceptibility, anti-tension strength of myocardial tissues, higher pro-inflammatory factor and mediator, and enhanced activation of matrix metalloproteinase [7, 8]. RhoA is one small molecule G protein, and participates in various intracellular signal transduction pathways in conjunction with its downstream effector molecule Rho kinase (ROCK). After AMI, RhoA/ROCK proteins in myocardial tissues were elevated and activated, for regulation of inflammatory and cell activity factors to participate in myocardial injury, cell apoptosis and myocardial fibrosis [9, 10]. ROCK exists in the form of two homologs, ROCK1 and ROCK2, both of which are expressed in vascular muscle and myocardial tissues. These information indicate the important role of RhA/ROCK signal pathway in the prognosis of AMI in aged mice. Fasudil is one RhoA/ROCK inhibitor, and can decrease
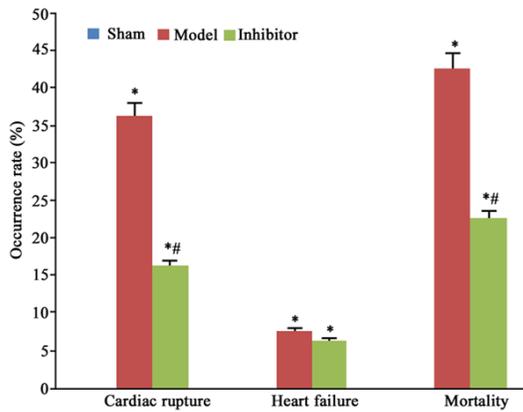
Figure 1. Rate of cardiac rupture and mortality in aged mice after AMI. *, P<0.05 compared to sham group; #, P<0.05 compared to model group.

the degree of myocardial fibrosis and infarction area in congestive heart failure rats, and alleviate inflammatory response after ischemia-reperfusion [11, 12]. This study thus established an AMI model in age mice, whose dynamic change of RhoA/ROCK signal pathway was observed, in an attempt to investigate the potential effect of RhoA/ROCK pathway inhibitor on cardiac rupture of AMI in aged mice and possible mechanism.

Materials and methods

Animals and grouping

Healthy male C57/BL mice (18 months, body weight 25~30 g) were provided by Laboratory Animal Center, Chinese Medicine Academy (Certificate number, SYXK-2013-0025) and were kept in an SPF grade facility with food and water *ad libitum*. Animals were randomly assigned into sham, AMI model and inhibitor groups (N=90 each). AMI model was established in mice from the latter two groups by ligating left coronary artery. RhoA/ROCK pathway inhibitor Fasudil (30 mg/kg/d) was applied via intraperitoneal injection. Equal volume of saline was introduced on sham and model groups.

Mice were used for all experiments, and all procedures were approved by the Animal Ethics Committee of Xi'an Central Hospital.

Drugs and reagents

RhoA/ROCK inhibitor Fasudil (30 mg in 2 ml, diluted in saline before use) was provided by Asahi Kasei Pharma Corp. Injection water (Ke-

lun Pharma, China); Pentobarbital and ketamine (Shanghai Chem, China). ELISA kits for interleukin-6 (IL-6) and tumor necrosis factor-α (TNF-α) were provided by Uscn (China). Rabbit anti-mouse ROCK1, RhoA, nuclear factor (NF)-κBp65 and transformation growth factor (TGF)-β1 were provide by Boster (China). Western blotting test kit was provided by Invitrogen (US). Horseradish peroxidase-conjugated goat anti-rabbit secondary antibody was purchased from CST (US).

AMI model

Mouse AMI model was generated by ligating left coronary artery as previously described [13]. Mice were anesthetized (atropine 1.2 mg/kg, xylazine 20 mg/kg and ketamine 100 mg/kg) and were fixed in left side clinostatism position. Tracheal intubation was performed for connecting ventilator. The chest cavity was opened via left ribs to ligate left coronary artery (using 6-0 suture). AMI model was deduced as whitening of ventricular anterior wall, weakened movement. After clearing hemorrhage inside the cavity, excess air was drained for suture. In sham group, coronary artery was separate but not ligated. 24 h after surgery, Fasudil (30 mg/kg/d) was applied via intraperitoneal injection. Equal volumes of saline were applied into the abdominal cavity in sham and model groups.

Drug delivery and observation of cardiac rupture

24 h after AMI model, Fasudil (30 mg/kg) was applied via intraperitoneal injection into inhibitor group daily for 14 consecutive days, while the other two groups received equal volume of saline. The survival rate of mice was monitored. 80 mice were chosen from model and inhibitor group for recording the rate of cardiac rupture 7 d after surgery. Those mice died within one week were dissected along with those sacrificed mice after 7 d. The cardiac rupture was deduced as abundant blood clot around the heart, or rupture of ventricular wall on infarction side. Cardiac failure was identified as severe heart expansion, large scale of infarction, pericardial effusion and pulmonary congestion.

Hemodynamic and cardiac ultrasound

HP 5500 colored Doppler ultrasonic apparatus was used to measure left ventricular end-dia-
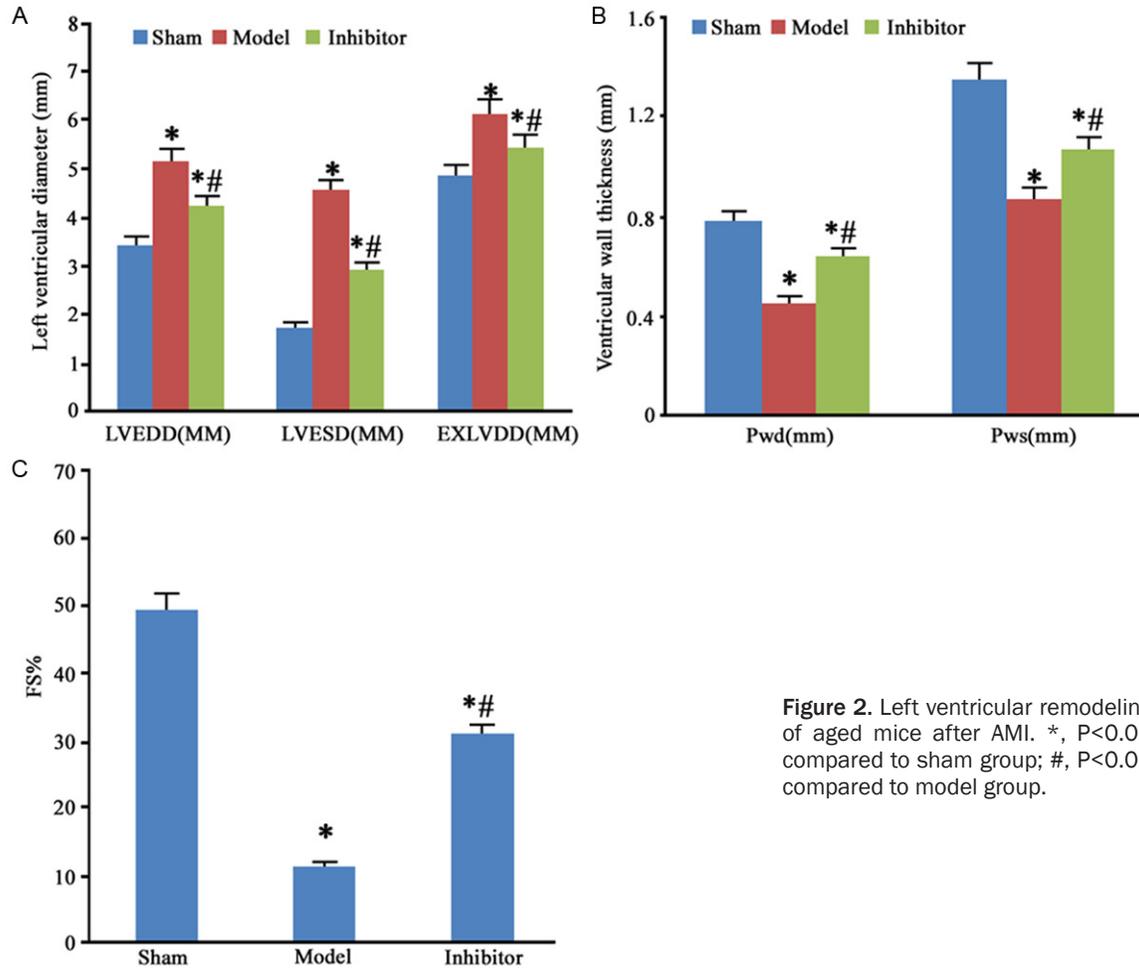
Figure 2. Left ventricular remodeling of aged mice after AMI. *, P<0.05 compared to sham group; #, P<0.05 compared to model group.

stolic diameter (LVEDD), left ventricular end-systolic diameter (LVESD), external diameter of left ventricular end-diastolic (EXLVDD) and ventricular wall thickness of diastolic/systolic phase (Pwd, Pws). Left ventricular fractional shortening (FS) = (LVEDD-LVESD)/LVEDD × 100%. An 1.4 F micro-cannula was inserted into ascending aorta and left ventricle via right common carotid artery to record blood pressure, left ventricular systolic pressure (LVSP), and maximal decreasing/increasing rate of internal pressure of left ventricle (dP/dt$_{min}$, dP/dt$_{max}$).

HE staining

HE staining was employed to detect the morphology of myocardial tissues. Eight animals were drawn from each group at day 7. Animals were sacrificed to extract myocardial tissues. After HE staining, the coverslip was mounted to observe tissue morphology under the light field microscope.

ELISA

ELISA was used to detect serum IL-6 and TNF-α levels from mouse serum samples following manual instruction. Absorbance values at 450 nm were recorded by a microplate reader in triplicates.

Western blotting

Western blotting was used to measure ROCK1, RhoA, NF-κBp65 and TGF-β1 expression in myocardial tissues. In brief, tissue samples were lysed in lysis buffer to collect the supernatant by centrifugation. The protein content was determined by BCA test kit. After SDS-PAGE separation, proteins were transferred to PVD membrane, which was blocked in buffer, mixed with primary antibody for 4°C overnight incubation. On the next day, the membrane was rinsed in TBST, and incubated in secondary antibody for 1 h. After TBST rinsing for three times, chromogenic substrate was added to develop the
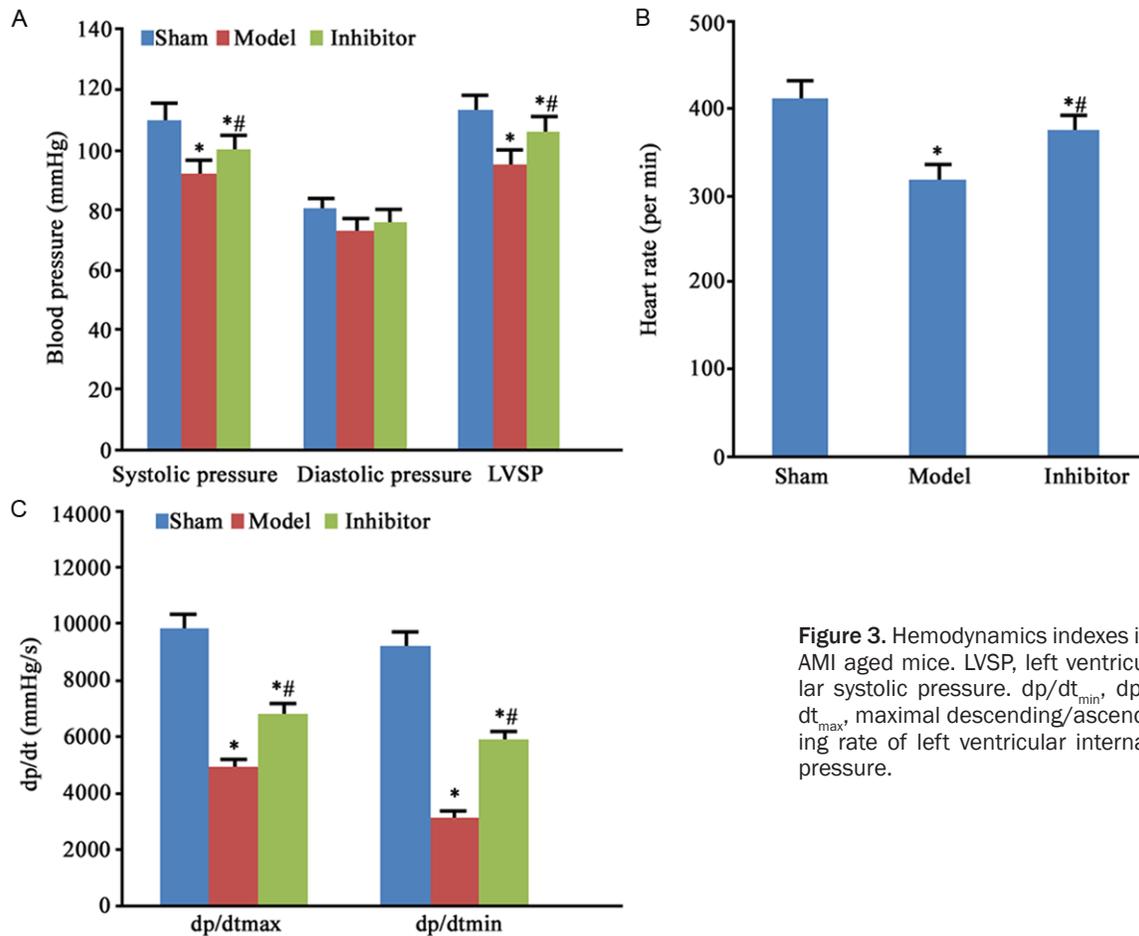
Figure 3. Hemodynamics indexes in AMI aged mice. LVSP, left ventricular systolic pressure. dp/dt$_{min}$, dp/dt$_{max}$, maximal descending/ascending rate of left ventricular internal pressure.

membrane, which was exposed in a dark room. Quantity One software was used to analyze protein bands, whose optical density was transformed into relative expression level, as the ratio between target protein and internal reference protein.

Statistical analysis

SPSS19.0 software was employed for data analysis. Using χ^2 test or corrected χ^2 test, we compare enumeration data. Those fitted the normal distribution were shown as mean ± standard deviation (SD). One-way analysis of variance (ANOVA) was used for compare means across multiple groups, followed by LSD test. A statistical significance was defined when P<0.05.

Results

Cardiac rupture rate of aged mice after AMI

After 3~6 d of cardiac rupture, inhibitor-treated mice had significantly lowered rate of cardiac

rupture compared to model group (χ^2=8.265, P<0.05). The overall mortality rate was also lower in treatment group (χ^2=7.293, P<0.05 compared to model group). No significant difference of the heart failure existed between those two groups (P>0.05, **Figure 1**).

Myocardial remodeling of left ventricle in AMI mice

Compared to sham group, the inner diameter of left ventricle was significantly increased in AMI model group, with expanded ventricular cavity (P<0.05) as well as significantly decreased FS, P$_{wd}$ and P$_{ws}$ (P<0.05). Inhibitor treatment significantly decreased inner diameter of left ventricle, ventricular cavity, and elevated FS, P$_{wd}$ and P$_{ws}$ (P<0.05 compared to model group, **Figure 2**).

Hemodynamic indexes of AMI mice

Compared to sham animals, model mice had significantly lowered heart rate, systemic sys-
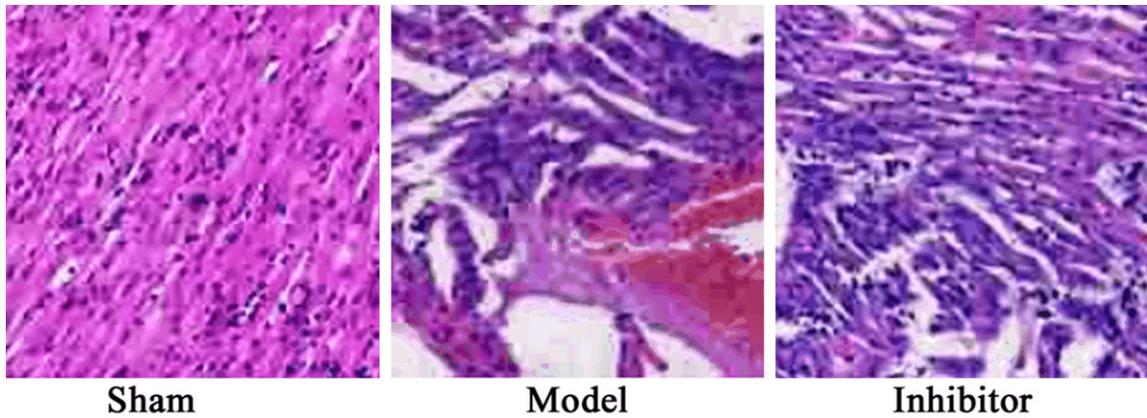
Figure 4. Myocardial morphology of aged mice after AMI (X200, HE staining).
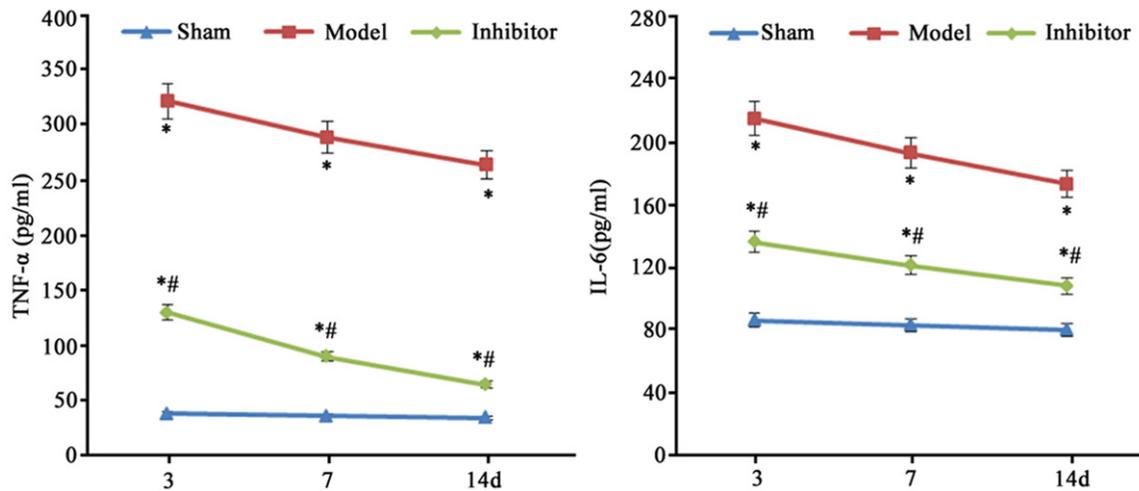
Figure 5. Serum IL-6 and TNF-α levels. *, P<0.05 compared to sham group; #, P<0.05 compared to model group.

tolic pressure and LVSP (P<0.05). Inhibitor treatment group had significantly elevated heart rate, systemic systolic pressure and LVSP (P<0.05, **Figure 3**).

Morphology of myocardial tissues after AMI

HE staining results showed no inflammatory infiltration in sham group, with tight and regular arrangement of myocardial cells. Model mice had more infiltration of inflammatory cells in myocardial tissues, with lower number of cells within the infarction area, accompanied with disarrangement of myocardial fiber, lysis or breakage. Inhibitor treatment group had alleviated inflammatory infiltration and regular arrangement of cells (**Figure 4**).

Serum IL-6 and TNF-α levels after AMI

Compared to sham group, AML model mice had significantly elevated serum IL-6 and TNF-α levels (P<0.05). With elongated time, serum IL-6 and TNF-α levels were gradually decreased. Inhibitor treated group had significantly depressed IL-6 and TNF-α levels (P<0.05 compared to model group, **Figure 5**).

Expression level of ROCK1, RhoA, NF-κBp65 and TGF-β1 proteins

Western blotting results showed elevated expression of ROCK1, RhoA, NF-κBp65 and TGF-β1 expression in AMI model mice (P<0.05 compared to sham group). With elongated time, expression levels of ROCK1, RhoA, NF-κBp65

Figure 6. Expression level of ROCK1, RhoA, NF-κBp65 and TGF-β1 in myocardial tissues.
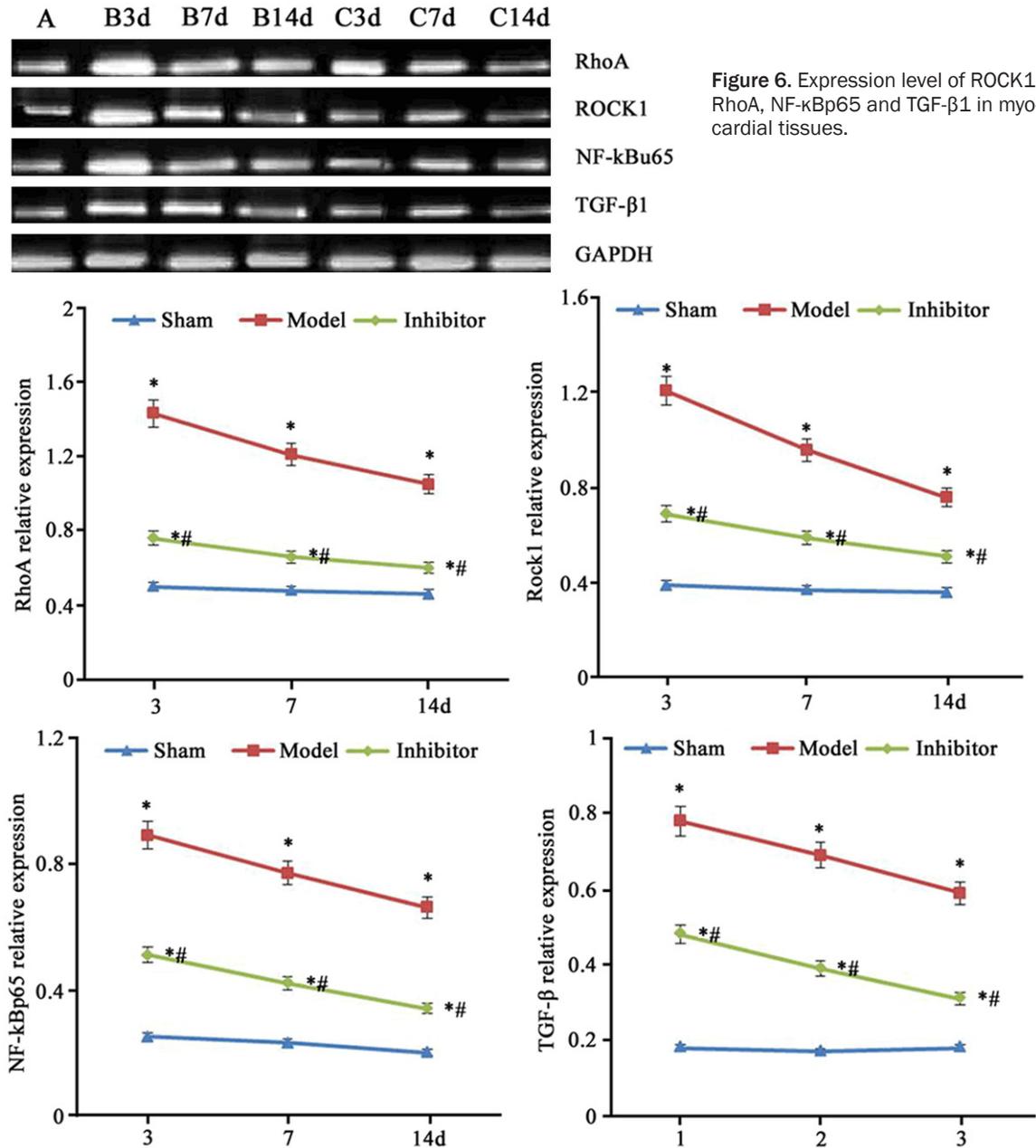
and TGF-β1 were gradually decreased. Compared to model group, inhibitor treated group had depressed ROCK1, RhoA, NF-κBp65 and TGF-β1 expression in myocardial tissues (P< 0.05, **Figure 6**).

Discussion

G protein coupled receptor and tyrosine kinase can activate RhoA, which regulates downstream effector molecule for mediating biological effects. Among those ROCK is the first dis-

covered downstream signal molecule. Rho binding domain of ROCK interacts with GTP-RhoA. The binding between arachidonic acid and PH domain of ROCK can activate ROCK [14, 15]. After receiving Rho activating signal, ROCK is activated to induce downstream phosphorylation/de-phosphorylation cascade reaction for mediating multiple biological effects. RhoA/ROCK thus plays an important role in pathology process after AMI. The ischemia-reperfusion injury and myocardial infarction-hypoxia damage can all lead to inflammatory

response. Previous study showed elevated expression of RhoA and ROCK signal proteins in myocardial tissues after ischemia-reperfusion injury, for mediating the expression of multiple inflammatory factors (interferon, interleukin) and infiltration/adhesion of inflammatory cells. By knocking down ROCK gene or suppressing ROCK activity, leukocyte adhesion can be depressed to decrease expression level of inflammatory factors; while Rho kinase inhibitor could reduce reactive injury of myocarditis [16, 17]. Myocardial fibrosis after infarction is related with bio-mechanical force or hemodynamic change, elevated extracellular matrix activity, oxidative stress or inflammatory response, which is caused by ischemia/hypoxia. The knockout of ROCK gene could reduce the proliferation rate of myocardial fibroblast in hypoxia-reperfusion mice, decrease the number of fibroblast precursor and fibroblast, and suppress the expression of pro-fibrosis cytokines [18, 19]. *In vitro* study has demonstrated that RhoA/ROCK signal pathway could facilitate mitochondria-mediated cell apoptosis via regulating the expression of apoptotic/anti-apoptotic proteins, and initiate exogenous cell apoptosis via TNF [20, 21].

Age is one risk factor for coronary heart disease. The incidence of cardiac death and AMI is elevated with elder people. Moreover, the probability of cardiac rupture is also higher in aged AMI patients, leaving its pathogenesis mechanism unclear [8]. This study observed the effect of RhoA/ROCK signal pathway on the rate of cardiac rupture in aged AMI mice, to investigate related mechanism of post-AMI cardiac rupture. Results showed the rupture time between 3 and 6 days post-AMI. Compared to model group, RhoA/ROCK inhibitor group had significantly lowered rate of cardiac rupture, along with lower overall mortality rate, suggesting that the inhibition of RhoA/ROCK signal pathway could reduce the cardiac rupture of AMI mice. 7 days after AMI, the inner diameter and cavity of left ventricle in model mice were significantly elevated, accompanied with lower FS%, P_{wd} and P_{ws}. RhoA/ROCK inhibitor mice had significantly decreased left ventricular inner diameter and cavity volume, along with higher FS%, P_{wd} and P_{ws}, and alleviated pathology injury of myocardial tissues, suggesting the important role of RhoA/ROCK signal pathway in improving ventricular remodeling after AMI for the cardiac rupture. After applying RhoA/ROCK signal pathway inhibitor, serum levels of inflammatory cytokines including IL-6 and TNF-α were remarkably decreased. Western blotting results showed elevated expression of ROCK1, RhoA, NF-κBp65 and TGF-β1 in myocardial tissues of model mice. With elongated time, expression levels of ROCK1, RhoA, NF-κBp65 and TGF-β1 were gradually decreased. Their expression levels were decreased in inhibitor group. Fasudil could block Rho kinase activity via competing for Rho kinase binding sites with ATP, to participate in various cellular pathways, suggesting the correlation between RhoA/ROCK signal pathway inhibitor-induced improvement of ventricular remodeling or decreasing cardiac rupture incidence with the suppression of RhoA/ROCK activity, lowered pro-inflammatory/pro-fibrotic factors. Such inhibitor could alleviate myocardial fibrosis and infiltration of inflammatory cells, to improve ventricular remodeling.

In summary, RhoA/ROCK pathway is probably related with post-AMI cardiac rupture. RhoA/ROCK inhibitor could suppress the activity of RhoA/ROCK pathway, down-regulate pro-inflammatory factor and pro-fibrotic factors, thus decreasing the rate of cardiac rupture.

Disclosure of conflict of interest

None.

Address correspondence to: Drs. Lina Hao and Chunping Kang, Department of Gerontology, Xi'an Central Hospital, No. 161 Xiwu Rd, Xi'an 710003, Shaanxi, China. Tel: +86-029-87268355; Fax: +86-029-87268355; E-mail: haolina220@sina.com (LNH); kangchunping220@sina.com (CPK)

References

[1] Bates ER. Reperfusion therapy reduces the risk of myocardial rupture complicating ST-elevation myocardial infarction. J Am Heart Assoc 2014; 3: e001368.

[2] Honda S, Asaumi Y, Yamane T, Nagai T, Miyagi T, Noguchi T, Anzai T, Goto Y, Ishihara M, Nishimura K, Ogawa H, Ishibashi-Ueda H, Yasuda S. Trends in the clinical and pathological characteristics of cardiac rupture in patients with acute myocardial infarction over 35 years. J Am Heart Assoc 2014; 3: e000984.

[3] Serpytis P, Karvelyte N, Serpytis R, Kalinauskas G, Rucinskas K, Samalavicius R, Ivaska J, Glaveckaite S, Berukstis E, Tubaro M, Alpert JS, Laucevičius A. Post-infarction ventricular septal defect: risk factors and early outcomes. Hellenic J Cardiol 2015; 56: 66-71.

[4] Rizza S, Copetti M, Cardellini M, Menghini R, Pecchioli C, Luzi A, Di Cola G, Porzio O, Ippoliti A, Romeo F, Pellegrini F, Federici M. A score including ADAM17 substrates correlates to recurring cardiovascular event in subjects with atherosclerosis. Atherosclerosis 2015; 239: 459-64.

[5] Soeda T, Higuma T, Abe N, Yamada M, Yokoyama H, Shibutani S, Ong DS, Vergallo R, Minami Y, Lee H, Okumura K, Jang IK. Morphological predictors for no reflow phenomenon after primary percutaneous coronary intervention in patients with ST-segment elevation myocardial infarction caused by plaque rupture. Eur Heart J Cardiovasc Imaging 2016; [Epub ahead of print].

[6] Hayano S, Takefuji M, Maeda K, Noda T, Ichimiya H, Kobayashi K, Enomoto A, Asai N, Takahashi M, Murohara T. Akt-dependent Girdin phosphorylation regulates repair processes after acute myocardial infarction. J Mol Cell Cardiol 2015; 88: 55-63.

[7] Zhu F, Li Y, Zhang J, Piao C, Liu T, Li HH, Du J. Senescent cardiac fibroblast is critical for cardiac fibrosis after myocardial infarction. PLoS One 2013; 8: e74535.

[8] Anderson DR, Poterucha JT, Mikuls TR, Duryee MJ, Garvin RP, Klassen LW, Shurmur SW, Thiele GM. IL-6 and its receptors in coronary artery disease and acute myocardial infarction. Cytokine 2013; 62: 395-400.

[9] Luo SY, Chen S, Qin YD, Chen ZW. Urotensin-Receptor Antagonist SB-710411 Protects Rat Heart against Ischemia-Reperfusion Injury via RhoA/ROCK Pathway. PLoS One 2016; 11: e0146094.

[10] Chen HC, Chang JP, Chang TH, Lin YS, Huang YK, Pan KL, Fang CY, Chen CJ, Ho WC, Chen MC. Enhanced expression of ROCK in left atrial myocytes of mitral regurgitation: a potential mechanism of myolysis. BMC Cardiovasc Disord 2015; 15: 33.

[11] Mera C, Godoy I, Ramírez R, Moya J, Ocaranza MP, Jalil JE. Mechanisms of favorable effects of Rho kinase inhibition on myocardial remodeling and systolic function after experimental myocardial infarction in the rat. Ther Adv Cardiovasc Dis 2016; 10: 4-20.

[12] Zhang J, Liu XB, Cheng C, Xu DL, Lu QH, Ji XP. Rho-kinase inhibition is involved in the activation of PI3-kinase/Akt during ischemic-preconditioning-induced cardiomyocyte apoptosis. Int J Clin Exp Med 2014; 7: 4107-14.

[13] Liu Z, Chen JM, Huang H, Kuznicki M, Zheng S, Sun W, Quan N, Wang L, Yang H, Guo HM, Li J, Zhuang J, Zhu P. The protective effect of trimetazidine on myocardial ischemia/reperfusion injury through activating AMPK and ERK signaling pathway. Metabolism 2016; 65: 122-30.

[14] Lee TM, Lin SZ and Chang NC. Membrane ERalpha attenuates myocardial fibrosis via RhoA/ROCK-mediated actin remodeling in ovariectomized female infarcted rats. J Mol Med (Berl) 2014; 92: 43-51.

[15] James SE, Burden H, Burgess R, Xie Y, Yang T, Massa SM, Longo FM, Lu Q. Anti-cancer drug induced neurotoxicity and identification of Rho pathway signaling modulators as potential neuroprotectants. Neurotoxicology 2008; 29: 605-12.

[16] Gao HC, Zhao H, Zhang WQ, Li YQ, Ren LQ. The role of the Rho/Rock signaling pathway in the pathogenesis of acute ischemic myocardial fibrosis in rat models. Exp Ther Med 2013; 5: 1123-1128.

[17] Guo J, Wang SB, Yuan TY, Wu YJ, Yan Y, Li L, Xu XN, Gong LL, Qin HL, Fang LH, Du GH. Coptisine protects rat heart against myocardial ischemia/reperfusion injury by suppressing myocardial apoptosis and inflammation. Atherosclerosis 2013; 231: 384-91.

[18] Rajapurohitam V, Izaddoustdar F, Martinez-Abundis E, Karmazyn M. Leptin-induced cardiomyocyte hypertrophy reveals both calcium-dependent and calcium-independent/RhoA-dependent calcineurin activation and NFAT nuclear translocation. Cell Signal 2012; 24: 2283-90.

[19] Martinez-Abundis E, Rajapurohitam V, Haist JV, Gan XT, Karmazyn M. The obesity-related peptide leptin sensitizes cardiac mitochondria to calcium-induced permeability transition pore opening and apoptosis. PLoS One 2012; 7: e41612.

[20] Moey M, Rajapurohitam V, Zeidan A, Karmazyn M. Ginseng (Panax quinquefolius) attenuates leptin-induced cardiac hypertrophy through inhibition of p115Rho guanine nucleotide exchange factor-RhoA/Rho-associated, coiled-coil containing protein kinase-dependent mitogen-activated protein kinase pathway activation. J Pharmacol Exp Ther 2011 339: 746-56.

[21] Soliman H, Nyamandi V, Garcia-Patino M, Varela JN, Bankar G, Lin G, Jia Z, MacLeod KM. Partial deletion of ROCK2 protects mice from high-fat diet-induced cardiac insulin resistance and contractile dysfunction. Am J Physiol Heart Circ Physiol 2015; 309: H70-81.